Effect of Preformed Correct Tertiary Interactions on Rapid Two-State Tendamistat Folding: Evidence for Hairpins as Initiation Sites for β-Sheet Formation†

Nancy Schönbrunner,‡ Günter Pappenberger,‡ Matthias Scharf,§ Joachim Engels,§ and Thomas Kiefhaber*,‡

Biozentrum der Universität Basel, Abteilung Biophysikalische Chemie, Klingelbergstrasse 70, CH 4056 Basel, Switzerland, and Institut für Organische Chemie der Universität Frankfurt, Marie Curie Strasse 11, D-60439 Frankfurt/Main, Germany

Received March 14, 1997; Revised Manuscript Received May 19, 1997⊗

ABSTRACT: The role of preformed correct side chain interactions, such as disulfide bonds, on protein folding kinetics is still not well understood. We investigated the effect of disulfide bond replacements on folding and stability of the small β-sheet protein tendamistat. Tendamistat folds very fast ($\tau = 10$ ms at pH 7 in water) and without detectable intermediates, which facilitates molecular interpretation of the kinetic data. Tendamistat contains two disulfide bonds, one between cysteines 11 and 27, which connects the ends of a β-hairpin, and a second one between cysteines 45 and 73, which brings together the two outer strands of a three-stranded β-sheet. Two single-disulfide variants of the protein were prepared by site-directed mutagenesis (tendamistat C11A/C27S and tendamistat C45A/C73A), and the effects on stability and on folding were monitored. Replacement of either disulfide bond leads to a large decrease in protein stability ($\Delta\Delta G^0 = 6.0$ kcal/mol for the C11A/C27S variant and 5.1 kcal/mol for the C45A/C73A variant). This effect is caused both by entropic stabilization of the unfolded state and by enthalpic destabilization of the native structure. Kinetic experiments show that the main effect of fixed side chain contacts is on the unfolding rate. For both single-disulfide variants, unfolding is strongly accelerated (4250 times in the C11A/C27S variant and 250 times in the C45A/C73A variant) whereas the refolding rate constants are only slightly decreased. The activation parameters show that the observed small effect on the refolding reaction in the C11A/C27S variant is a consequence of large and compensating changes in the entropy and enthalpy of activation. Structural interpretation of the kinetic data suggests that formation of the β-hairpin stabilized by the C11−C27 disulfide bond forms in the rate-limiting step of the refolding process. The interactions between the outer strands of the β-sheet connected by the C45−C73 disulfide bond, in contrast, are made late in refolding. These results support the idea that β-hairpins are initiation sites for β-sheet formation and that additional strands are added late in the folding process.

Recent theoretical and experimental results on the mechanism of protein folding have initiated a discussion on the role of the frequently observed partially folded states [for an overview, see Baldwin (1995)] and led to the revival of the nucleation/growth model, popular in the 1970's before equilibrium and kinetic intermediates were characterized (Tsong et al., 1972; Wetlaufer, 1973). According to the nucleation/growth model, the rate-limiting step occurs early in folding and reflects the formation of a nucleated state, which may be a high-energy intermediate. All further steps, which may include the successive formation of intermediate structures, occur much more rapidly and can thus not be detected in kinetic folding experiments. The nucleation model was recently supported by site-directed mutagenesis work on chymotrypsin inhibitor 2 (Itzhaki et al., 1995) and by direct measurement of nucleation and growth rates for formation of a kinetically trapped intermediate in lysozyme folding (Kiefhaber et al., 1997). It is further consistent with a large number of theoretical studies on protein folding (Thirumalai, 1994; Abkevich et al., 1994; Wolynes et al., 1995). Additional evidence against the importance of populated intermediate states for protein folding recently came from folding studies on a number of small proteins, which fold very rapidly and without transient accumulation of partially folded states (Jackson & Fersht, 1991; Alexander et al., 1992; Viguera et al., 1994; Huang & Oas, 1995; Schindler et al., 1995; Villegas et al., 1995; Schönbrunner et al., 1997).

We use the small (74 amino acid) α-amylase inhibitor tendamistat, from *Streptomyces tendae*, as a model system to study the mechanism of protein folding. Tendamistat contains only β-sheets and turns as secondary structural elements, and it possesses two disulfide bonds (Kline & Wüthrich, 1985; Pflugrath et al., 1986; Kline et al., 1988). We showed recently that the folding and unfolding reactions of tendamistat (disulfide bonds intact) exhibit strict two-state behavior (Schönbrunner et al., 1997). Up to now it represents the only case of a disulfide-bonded protein which folds in a two-state manner. The use of model proteins which exhibit two-state folding and unfolding kinetics to study protein folding allows investigation of the direct folding process from the unfolded state to the native structure. Further, the molecular interpretation of results from site-directed mutagenesis on kinetic two-state systems is facilitated, since the effect of the mutagenesis on the stability of folding intermediates is eliminated. Tendamistat thus pro-

† This work was supported by a grant from the Schweizerische Nationalfonds.

* To whom correspondence should be addressed. Phone: ++41-61-267-2194. Fax: ++41-61-267-2189. E-mail: kiefhaber@ubaclu.unibas.ch.

‡ Biozentrum der Universität Basel.

§ Institut für Organische Chemie der Universität Frankfurt.

⊗ Abstract published in *Advance ACS Abstracts,* July 1, 1997.

S0006-2960(97)00594-1 CCC: $14.00

vides an excellent model system (a) to elucidate the rate-limiting steps in β-sheet formation during protein refolding and (b) to investigate the role of preformed correct tertiary contacts for the mechanism and the rate of protein folding.

Up to date, very little data are available on the folding of all β-sheet proteins. In contrast to α-helices, which are known to be able to form very rapidly (Gruenewald et al., 1979; Williams et al., 1996), β-sheets represent mainly nonlocal structures and thus require specific interactions between distant parts of the polypeptide chain. Theoretical models predict that the process of β-sheet formation is initiated at β-hairpin structures, which involve adjacent strands and thus represent nearest-neighbor interactions in β-sheets (Finkelstein, 1991). Sheet propagation is believed to occur by addition of further strands. The rate-limiting step in β-sheet formation was proposed to be the formation of a few specific interactions within the first β-hairpin. The following propagation reactions are predicted to occur fast.

The influence of preformed disulfide bonds on protein folding kinetics has been widely discussed in recent years. It has been speculated that intact disulfide bonds may give rise to kinetically trapped intermediates during protein refolding (Chaffotte et al., 1992). The results on wild-type tendamistat folding showed, however, that rapid two-state folding can occur in disulfide-intact proteins (Schönbrunner et al., 1997). Other models argued that intact disulfide bonds enhance the rate of protein folding by restricting the conformational space for the folding polypeptide chain (Flory, 1956; Camacho & Thirumalai, 1995) and by acting as seeds for correct tertiary structure. Experimental studies on the role of disulfide bonds in folding of oxidized proteins suggested that preformed disulfide bonds can slow down unfolding and refolding reactions (Lin et al., 1985; Denton et al., 1994; Mücke & Schmid, 1994). However, folding of the model proteins used in these studies was slow and involved trapped intermediates and/or prolyl isomerization reactions. Thus, the influence of preformed tertiary interactions on the actual folding process is still not well understood.

Here we report studies on two single-disulfide mutants of tendamistat to investigate the mechanism of β-sheet formation and to elucidate the role of preformed correct tertiary contacts in the process of protein folding. In the classical mutagenesis experiments introduced by Fersht and coworkers (Fersht et al., 1992), it is assumed that the structure of the unfolded state is not affected by mutations. Thus, the difference between the wild-type protein and the variants arises solely from altered side chain interactions in the transition state and/or in the native state. In the case of disulfide bond replacements, we observe that the unfolded state becomes significantly more solvent-accessible upon replacement of each of the two disulfide bonds. This gives us the unique opportunity to additionally monitor the disappearance of the increased solvent accessibility during protein folding, and it allows the measurement of the degree of compactization in different regions of the protein in the transition state of folding. The results show that the β-hairpin between residues 12 and 26 is formed in the rate-limiting step of the folding process, supporting the idea that formation of hairpin structures represents the rate-limiting step in β-sheet formation (Finkelstein, 1991). The contacts between the outer strands of the second β-sheet, in contrast, are only formed late in the folding process. Comparison of the folding rates of the mutants with the wild-type protein shows that each of the preformed disulfide bonds enhances the rate of the folding reaction only slightly, but it leads to a strong decrease in the unfolding rate constants by enthalpic stabilization of the native state. Interestingly, even cross-linking the base of the β-hairpin comprised by strands I and II of the first β-sheet, which forms in the transition state, increases the rate of tendamistat folding only slightly. This effect is due to large and compensating effects on the entropy and enthalpy of activation.

MATERIALS AND METHODS

Materials

Tendamistat was expressed and isolated according to Vértesy et al. (1984). The disulfide-deficient mutants (C11A/C27S and C45A/C73A)[1] were constructed, expressed in *Steptomyces lividans*, and purified as described by Haas-Lauterbach et al. (1993). Protein concentration was determined by UV absorption measurements using an absorption coefficient $A_{280}^{0.1\%} = 1.61$ for wild-type and mutant proteins (Vértesy et al., 1984).

Ultrapure GdmCl (AA grade) was from Nigu Chemie (Waldkraiburg, Germany) and was used without further purification. All other chemicals were reagent grade and were purchased from Merck (Darmstadt, Germany).

Methods

Equilibrium Unfolding Transitions. The GdmCl-induced equilibrium transitions of tendamistat were monitored by the change in ellipticity at 227 nm in an Aviv 62A DS spectropolarimeter. The positive band in this wavelength region for the native protein is probably caused by the disulfide bonds (Vogl et al., 1995). Both single-disulfide variants show a slightly weaker band at this position (cf. Figure 2A).

Native protein (in 100 mM cacodylic acid, pH 7.0) was diluted into the same buffer containing the appropriate concentration of GdmCl and incubated at 25 °C for 1 h. The final protein concentration was 0.1 mg/mL, and the ellipticity was measured in a 1 cm cell in a temperature-controlled cuvette holder. The data were analyzed assuming a two-state transition. The complete unfolding curve was fitted according to the equation of Santoro and Bolen (1988) to yield values for ΔG^0 and its [GdmCl] dependence ($m_{eq} = d\Delta G^0/d[GdmCl]$). Reversibility was checked by diluting completely unfolded protein into appropriate concentrations of GdmCl which gave identical values as starting from native protein.

GdmCl Dependence of the Folding and Unfolding Reaction. The GdmCl dependence of the refolding and unfolding reaction was monitored by diluting completely unfolded protein (wild type in 5.5 M GdmCl, 10 mM Gly/HCl, pH 2; tendamistat C11A/C27S in 2.5 M GdmCl, 100 mM cacodylic acid, pH 7; tendamistat C45A/C73A in 3.5 M GdmCl, 100 mM cacodylic acid, pH 7) or completely native protein (wild type in 5.0 M GdmCl and tendamistat C11A/C27S and

[1] Abbreviations: CD, circular dichroism; GdmCl, guanidinium chloride; λ, apparent rate constant ($=1/\tau$); NMR, nuclear magnetic resonance; tendamistat C11A/C27S, tendamistat variant with amino acids Cys11 and Cys27 replaced by alanine and serine, respectively; tendamistat C45A/C73A, tendamistat variant with amino acids Cys45 and Cys73 each replaced by alanine.

C45A/C73A in 0 M GdmCl, 100 mM cacodylic acid, pH 7) into the appropriate concentration of GdmCl in 100 mM cacodylic acid at 25 °C. The final pH was 7.0, and protein concentrations were 0.03 mg/mL. Fast reactions (τ < 10 s) were monitored by the change in fluorescence above 320 nm after excitation at 276 nm using stopped-flow mixing in an Applied Photophysics SM-17MV instrument with a fixed mixing ratio of 1 + 10 (11-fold dilution). The reaction at each particular GdmCl concentration was repeated at least 4 times with almost identical amplitudes and rate constants (±10%). The average of the kinetic traces was used for data analysis. Slow reactions (τ > 10 s) were additionally measured by manual mixing and monitored by the change in fluorescence at 345 nm after excitation at 276 nm in a Hitachi F-4500 fluorometer. Under conditions where the reactions could be measured by manual and by stopped-flow mixing, both methods gave identical rate constants.

The temperature dependence of the refolding and the unfolding reactions was measured as described above while varying the temperature from 5 to 45 °C. The data were extrapolated to 0 M GdmCl by measuring refolding and unfolding reactions at different concentrations of GdmCl at the individual temperatures. At the extreme temperatures, the apparent rate constants (λ) were determined over the complete range of GdmCl concentrations to check for deviations from the two-state behavior. At all temperatures, the slopes of the GdmCl dependence of ln k_f and ln k_u were essentially linear, indicating the validity of the two-state model. Unfolding of the wild-type protein could only be measured over a narrow temperature range (20−37 °C), since the protein becomes too stable and will not unfold completely at temperatures below 20 °C.

Transition State Analysis. The free energies of activation for folding/unfolding ($\Delta G^{0\ddagger}_{f,u}$) were calculated using transition state theory according to Eyring (1935):

$$k = \frac{\kappa k_b T}{h} \exp\left[-\left(\frac{\Delta G^{0\ddagger}}{RT}\right)\right] \quad (1)$$

where k_b is the Boltzmann constant, T is the absolute temperature in degrees kelvin, h is Planck's constant, and R is the gas constant. κ is the transmission factor which has an upper limit of 1. Alternative considerations suggest that the preexponential factor is considerably smaller for reactions in solution (Kramers, 1940) and especially for protein folding reactions (Chan et al., 1996), leading to a decrease in the absolute value of the free energy of activation. However, application of the Eyring formalism is still warranted for comparison of $\Delta G^{0\ddagger}$ values of the wild-type protein and of the mutants if the preexponential factor does not change upon mutation. The given values of $\Delta G^{0\ddagger}$ should therefore be regarded as apparent free energies of activation.

For determination of the folding (k_f) and unfolding rate constants (k_u) at 0 M GdmCl, the following relations were used (Tanford, 1970):

$$\ln k_f = \ln k_f(H_2O) + m'_f[\text{denaturant}] \quad (2)$$

$$\ln k_u = \ln k_u(H_2O) + m'_u[\text{denaturant}] \quad (3)$$

Using eq 1, the rate constants can be converted into apparent free energies of activation:

$$\Delta G^{0\ddagger}_f = \Delta G^{0\ddagger}_f(H_2O) + m_f[\text{denaturant}] \quad (4)$$

$$\Delta G^{0\ddagger}_u = \Delta G^{0\ddagger}_u(H_2O) + m_u[\text{denaturant}] \quad (5)$$

with $m_f = d\Delta G^{0\ddagger}_f/d[\text{denaturant}]$ and $m_u = d\Delta G^{0\ddagger}_u/d[\text{denaturant}]$. For two-state reactions as observed in tendamistat folding (Schönbrunner et al., 1997)

$$U \underset{k_u}{\overset{k_f}{\rightleftharpoons}} N \quad (6)$$

the apparent rate constant (λ) is the sum of k_u and k_f:

$$\lambda = k_f + k_u \quad (7)$$

The complete GdmCl dependence of λ was fitted in a single step according to

$$\ln \lambda = \ln [k_f(H_2O)\, e^{-m'_f[\text{denaturant}]} + k_u(H_2O)\, e^{-m'_u[\text{denaturant}]}] \quad (8)$$

The obtained values of k_f, k_u, m'_f, and m'_u were converted into the respective values of $\Delta G^{0\ddagger}_f$, $\Delta G^{0\ddagger}_u$, m_u, and m_f according to eqs 1−3. These values were compared to ΔG^0_{eq} and m_{eq} obtained from equilibrium transition curves:

$$\Delta G^0_{eq} = \Delta G^{0\ddagger}_f - \Delta G^{0\ddagger}_u \quad (9)$$

$$m_{eq} = m_f - m_u \quad (10)$$

The ratio of m_f/m_{eq} was used as a measure for the degree of exposure of the transition state to solvent.

Temperature Dependence of Rates of Refolding. The activation enthalpy ($\Delta H^{0\ddagger}$) and entropy ($\Delta S^{0\ddagger}$) of a reaction depend on temperature according to

$$\Delta H^{0\ddagger}(T) = \Delta H^{0\ddagger}(T^0) + \Delta C_p^{\ddagger}(T - T^0) \quad (11)$$

$$\Delta S^{0\ddagger}(T) = \Delta S^{0\ddagger}(T^0) + \Delta C_p^{\ddagger} \ln (T/T^0) \quad (12)$$

where $\Delta C_p^{\ddagger}$ is the change in heat capacity upon formation of the transition state. T^0 is the reference temperature (298.15 K), and $\Delta S^{0\ddagger}(T^0)$ and $\Delta H^{0\ddagger}(T^0)$ are the changes in entropy and enthalpy of activation at that temperature. $\Delta S^{0\ddagger}_f(T)$ and $\Delta H^{0\ddagger}_f(T)$ are the entropy and enthalpy of activation at any given temperature T. These relations cause a curvature in the temperature dependence of the activation free energy of the refolding and unfolding according to

$$\Delta G^{0\ddagger}(T) = \Delta H^{0\ddagger}(T^0) - T\Delta S^{0\ddagger}(T^0) + \Delta C_p^{\ddagger}[T - T^0 - T \ln (T/T^0)] \quad (13)$$

Substitution of eq 14 into eq 1 and rearrangement provide an expression for the temperature dependence of rate constants (k):

$$\ln \frac{k}{T} = \ln \frac{\kappa k_b}{h} - \frac{1}{RT}\{\Delta H^{0\ddagger}(T^0) - T\Delta S^{0\ddagger}(T^0) + \Delta C_p^{\ddagger}[T - T^0 - T \ln (T/T^0)]\} \quad (14)$$

It should be noted that the obtained values for $\Delta H^{0\ddagger}$ represent the actual enthalpy of activation whereas the

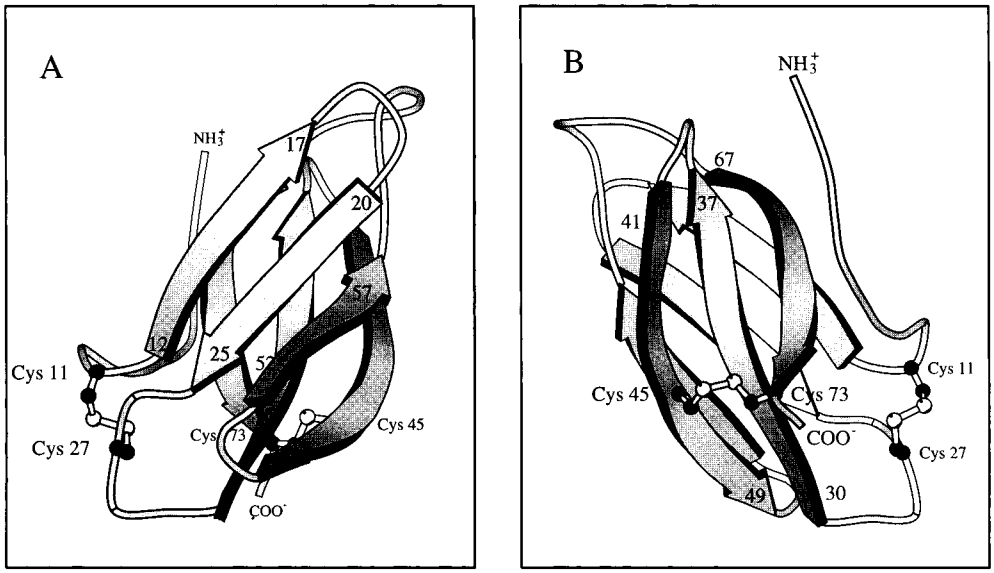

FIGURE 1: Schematic representation of the structure of tendamistat. The disulfides are shown as ball and stick models. The disulfide bond between Cys11 and Cys27 is located at the base of the hairpin between residues 12 and 26 (strands 1 and 2; panel A). The disulfide bond between Cys45 and Cys73 connects strands IV and VI (panel B). The figure was drawn using the program Molscript (Kraulis, 1991).

obtained values for $\Delta S^{0\ddagger}$ represent an apparent entropy of activation due to the uncertainty of the preexponential factor in eq 1.

Data Fitting. For data fitting, the programs KaleidaGraph (Applebeck Software), KinFit (Olis), and ProFit (Cherwell Scientific Ltd.) and the software provided with the Applied Photophysics stopped-flow instrument were used.

RESULTS

Replacement of Disulfide Bonds. The structure of tendamistat is known at high resolution both in the crystal (Pflugrath et al., 1986) and in solution (Kline et al., 1988; Figure 1). The two disulfide bonds in tendamistat are found between residues 11 and 27 and between residues 45 and 73. The 11−27 disulfide bond is located at the base of a β-hairpin formed by strands I and II of the first β-sheet (Figure 1A). The loop connecting the two strands of this hairpin contains the single tryptophan residue in the molecule, which is solvent exposed and which determines the fluorescence properties of the molecule.

The 45−73 disulfide bond is located between strands IV and VI, the two outer strands of the second β-sheet (Figure 1B). It thus connects more distant structural elements than the 11−27 disulfide bond. It may be viewed as a probe of the completeness of the formation of the second β-sheet.

In our studies, we used two single-disulfide variants of tendamistat. One has the cysteine residues at positions 45 and 73 replaced by alanines (C45A/C73A), and the other one has cysteine residues 11 and 27 replaced by alanine and serine, respectively (C11A/C27S). Replacement of both disulfide bonds simultaneously did not yield native protein, due to largely reduced protein stability.

The structure of the native state of both disulfide variants appears to be identical to that of the wild type based on tryptophan fluorescence, near- and far-UV CD spectra, the absorption spectrum, and inhibitory activity (data not shown). Recently, the solution structure of the C45A/C73A variant was determined by heteronuclear 2-D NMR spectroscopy, and it was shown to be identical to that of the wild-type protein (Balbach, Kessler, and Engels, unpublished results). The NMR assignments of the C11A/C27S variant are currently in progress.

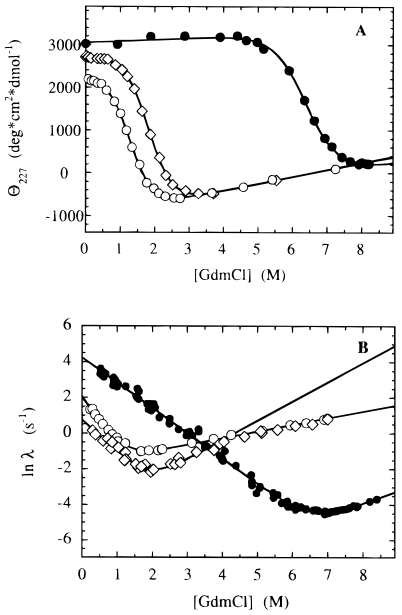

FIGURE 2: (A) GdmCl-induced unfolding transition at pH 7.0, 25 °C, monitored by the change in ellipticity at 227 nm for wild-type tendamistat (●), C45A/C73A (◇), and C11A/C27S (○). The line represents the least-squares fit assuming the two-state model (Santoro & Bolen, 1988). The parameters from the fits are shown in Table 1. (B) [GdmCl] dependence of the apparent rate constants for refolding and unfolding (λ) for wild-type tendamistat (●), C45A/C73A (◇), and C11A/C27S (○) monitored by the change in tryptophan fluorescence under the same solvent conditions as in panel A. The data were fit according to eq 9. The parameters from the fits are also shown in Table 1.

Effect of Disulfide Bonds on Tendamistat Stability. A comparison of the GdmCl-induced unfolding transitions for wild-type tendamistat and the two single-disulfide variants is shown in Figure 2A. The transitions were monitored by the change in the CD signal at 227 nm. The removal of each disulfide bond leads to a large loss in stability. Table 1 shows that the effect is stronger for the replacement of

Table 1: Kinetic and Equilibrium Parameters for Tendamistat Folding[a]

tendamistat variant	$\Delta G^{0\ddagger}_{f}$ (kcal/mol)	m_f [(kcal/mol)/M]	$\Delta G^{0\ddagger}_{u}$ (kcal/mol)	m_u [(kcal/mol)/M]	ΔG^{0}_{f-u} (kcal/mol)	m_{f-u} [(kcal/mol)/M]	ΔG^{0}_{eq} (kcal/mol)	m_{eq} [(kcal/mol)/M]
wild type	14.95 ± 0.26	-0.83 ± 0.03	23.36 ± 0.74	0.45 ± 0.02	-8.28 ± 1.0	1.28 ± 0.05	-8.13 ± 0.16	1.27 ± 0.02
C11A/C27S	16.24 ± 0.24	-1.65 ± 0.06	18.49 ± 0.03	0.22 ± 0.003	-2.12 ± 0.27	1.87 ± 0.07	-2.29 ± 0.14	1.79 ± 0.06
C45A/C73A	17.00 ± 0.09	-1.07 ± 0.10	20.22 ± 0.25	0.64 ± 0.09	-3.09 ± 0.34	1.71 ± 0.19	-3.10 ± 0.13	1.70 ± 0.06

[a] The equilibrium (eq) values were determined by fitting the GdmCl-induced transition curves shown in Figure 2A according to the two-state model (Santoro & Bolen, 1988). The kinetic parameters for the folding (f) and unfolding (u) reactions are the result of nonlinear least-squares fits of the data shown in Figure 2B to eq 8. Values for $\Delta G^{0\ddagger}_{u,f}$ were determined from the fitted rate constants for folding and unfolding (k_f and k_u, respectively) using eq 1. All parameters are given for pH 7.0, 25 °C.

the C11−C27 disulfide bond ($\Delta\Delta G^0 = 6.0$ kcal/mol) than for the C45−C73 bond ($\Delta\Delta G^0 = 5.1$ kcal/mol).

In addition to the changes in stability, both variants show markedly increased m_{eq} values compared to the wild-type protein ($m_{eq} = d\Delta G^0/d[\text{GdmCl}]$; Table 1). The effect is similar both for the C11A/C27S variant [$\Delta m_{eq} = m_{eq}(\text{wt}) - m_{eq}(\text{mu}) = -0.55$ (kcal/mol)/M] and for the C45A/C73A variant [$\Delta m_{eq} = -0.42$ (kcal/mol)/M]. The increased m values in the single-disulfide variants indicate the loss of residual structure in the unfolded state and thus point to a higher degree of solvent accessibility in the unfolded state of the mutants.

It is apparent from Figure 2A that the choice of conditions (pH 7.0, 25 °C) is well-suited for comparison studies. Under these conditions, the unfolding of the wild-type protein can still be measured completely, while both mutants are still native in the absence of GdmCl. Errors in the thermodynamic analysis of the unfolding transitions arise from the scarcity of native base line for the single-disulfide variants and scarcity of unfolded base line for the wild-type proteins.

Effect of Disulfide Bonds on Tendamistat Folding Kinetics. Figure 2B compares the GdmCl dependence of the apparent folding rate constants (λ) of wild-type tendamistat and of the two single-disulfide variants. The GdmCl dependence of the folding reaction was analyzed according to the two-state model (Schönbrunner et al., 1997) with $\lambda = k_u + k_f$, assuming linear GdmCl dependencies of ln k_u and ln k_f (Aune & Tanford, 1969). The values of $\Delta G^{0\ddagger}_{u}$ and $\Delta G^{0\ddagger}_{f}$ were calculated from the extrapolated unfolding and refolding rate constants at 0 M GdmCl according to transition state theory by Eyring (1935; eq 1). The resulting values and their GdmCl dependencies are given in Table 1. For both variants, the m values and the ΔG^0 values calculated from the kinetic parameters agree well with the respective values from equilibrium transition curves. This shows that the two-state character of the folding and unfolding reactions is not changed by the disulfide bond replacements. Interestingly, the unfolding limb of the C45A/C73A mutant displays a prominent kink at 4 M GdmCl, which is observed neither for the wild-type protein nor for the C11A/C27S variant. Comparing the kinetic data below 4 M GdmCl with the respective data from the equilibrium transition (Figure 2) leads to identical values for ΔG^0 and m_{eq} (Table 1). The shallower slope of ln λ at higher concentrations of GdmCl probably reflects a change in the unfolding mechanism. This phenomenon will be discussed elsewhere (Pappenberger and Kiefhaber, manuscript in preparation).

As in the wild-type protein, an additional slow refolding pathway exists in the single-disulfide variants. On this pathway, 20% of the unfolded molecules reach the native state slowly ($\tau = 10$ s) in a prolyl isomerization limited reaction. Since tendamistat folding is faster than prolyl isomerization and only *trans* Xaa−Pro peptide bonds are present in the native structure, this reaction does not influence the analysis of the actual folding reaction (Kiefhaber et al., 1992). It is omitted in Figure 2B for clarity.

As expected from the equilibrium transition curves (Figure 2A), the minimum of the folding rate constants for both single-disulfide variants is located at much lower GdmCl concentrations than for the wild-type protein. In all cases, the minimum of the rate constants corresponds to the midpoint of the GdmCl-induced equilibrium unfolding transitions. It can be seen in Figure 2B that the unfolding rates are strongly enhanced for both single-disulfide variants compared to the wild-type protein. The C45A/C73A variant unfolds 250 times faster and the C11A/C27S variant unfolds 4250 times faster extrapolated to 0 M GdmCl. The rate of the refolding reaction is only slightly decreased in both single-disulfide variants compared to the wild-type protein (30-fold for the C45A/C73A variant and 8-fold for the C11A/C27S protein). The GdmCl dependencies of the refolding rate and unfolding rate constants (m values) are also changed in both mutants compared to the wild-type protein. The most significant effect is observed for the folding of the C11A/C27S variant. Here the refolding reaction depends much stronger and the unfolding reaction much weaker on the GdmCl concentration than in the wild-type protein (Figure 2B and Table 1).

Accessibility Changes during Tendamistat Refolding. The increased m values of the single-disulfide variants offer a unique opportunity to monitor the relative accessibility of different parts of the protein in the transition state of folding. The values of Δm_u [$= m_u(\text{wt}) - m_u(\text{mutant})$] and Δm_f [$= m_f(\text{wt}) - m_f(\text{mutant})$] were compared to the overall change in m value between the wild-type and the variants in the same way as the changes in free energy are used to calculate ϕ values (Fersht et al., 1992; see below). These data were used to calculate α values ($= -\Delta m_f/\Delta m_{eq}$). α values should give detailed information on the degree of accessibility in certain regions of the protein in the transition state for folding. The regions which can be monitored are those which are forming nonrandom structure in the unfolded state when the disulfide bond is intact. The native state was chosen as reference state, since the disulfide replacements were assumed to have larger effects on the solvent accessibility of the unfolded state compared to the native structure. Table 2 gives the α values for the two single-disulfide variants. The two variants show different behavior. For the C45A/C73A variant, 55% of accessibility gain upon mutation is lost in the transition state of folding ($\alpha = 0.55$) whereas for the C11A/C27S variant more than the accessibility gained in the unfolded state upon mutation is lost in the transition state of folding ($\alpha = 1.39$). Consequently, less change in solvent accessibility occurs between the transition state and the native state, for the

Table 2: ϕ and α Values for Single-Disulfide Tendamistat Variants[a]

tendamistat variant	$\phi_{U\ddagger}$	$\alpha_{U\ddagger}$
C11A/C27S	0.21	1.39
C45A/C73A	0.39	0.55

[a] ϕ values were calculated from the ΔG^0 values given in Table 1 using $\phi_{U\ddagger}$ [$=\Delta\Delta G^{0\ddagger}_f$(wt-mutant)/$\Delta\Delta G^0$(wt-mutant)]. α values are defined as $\alpha = \Delta m_f$(wt-mutant)/Δm_{eq}(wt-mutant). α values were calculated using the data given in Table 1. They indicate what fraction of the increase in solvent accessibility of the unfolded state in the disulfide variant is lost in the transition state of folding.

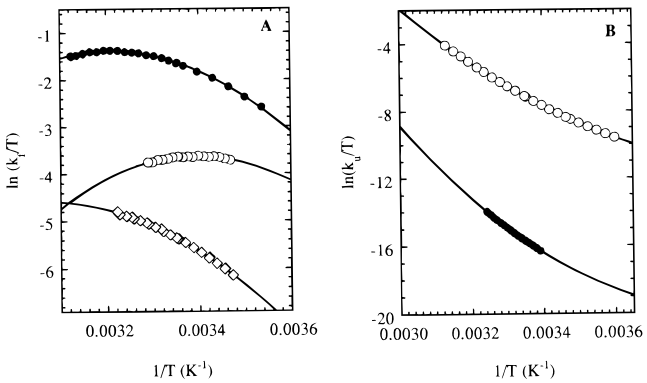

FIGURE 3: Temperature dependence of (A) the refolding rate constants (k_f) and (B) the unfolding rate constants (k_u) at pH 7.0 extrapolated to 0 M GdmCl for wild-type tendamistat (●), C45A/C73A (◇), and C11A/C27S (○), shown as Eyring plots. Nonlinear least-squares fits of the curves to eq 15 yield the parameters given in Table 3.

C11A/C27S variant compared to the wild-type protein.

Energy Changes during Tendamistat Folding. To assess the energy changes occurring during the refolding and unfolding of the tendamistat variants, we followed the method introduced by Fersht and co-workers (Fersht et al., 1992) and calculated values of $\phi_{U\ddagger}$ [$=\Delta\Delta G^{0\ddagger}_f$(wt-mutant)/$\Delta\Delta G^0$(wt-mutant)], which represents the relative change in free energy occurring in the folding reaction (Table 2). A value of 1 for $\phi_{U\ddagger}$ indicates that the change in free energy introduced by the mutation is also present in the transition state. Consequently, this interaction is already completely formed in the transition state of folding. A $\phi_{U\ddagger}$ value of 0, in contrast, indicates that the interaction is completely absent in the transition state and is formed after the rate-limiting step in refolding. Both disulfide variants of tendamistat have ϕ values in between these extremes. The C11A/C27S variant has a ϕ value of 0.21, and the C45A/C73A variant has a ϕ value of 0.39.

Temperature Dependence of Tendamistat Folding. The results from the accessibility changes during tendamistat folding showed that in the case of disulfide replacements the transition state can change in its position on the reaction coordinate. This effect is particularly pronounced for the C11A/C27S variant, and it obstructs the molecular interpretation of the changes in $\Delta G^{0\ddagger}$. We therefore determined the activation parameters for all three tendamistat variants to assess the thermodynamic properties of their transition states relative to the unfolded state and to the native state.

Refolding kinetics for all three variants were measured at various temperatures. This allows analysis of the data using Eyring plots (Figure 3A, eq 14) which give $\Delta H^{0\ddagger}$, $\Delta S^{0\ddagger}$, and $\Delta C_p^{\ddagger}$. Table 3 shows the contributions of $\Delta H^{0\ddagger}_f$ and $T\Delta S^{0\ddagger}_f$ to the observed $\Delta G^{0\ddagger}_f$ for the wild-type protein and for both single-disulfide variants. The most dramatic change occurs in the C11A/C27S variant at 25 °C. Here $T\Delta S^{0\ddagger}_f$ decreases from −8.36 kcal/mol in wild-type to −18.07 kcal/mol in the variant. However, this decrease in $T\Delta S^{0\ddagger}_f$ is compensated for by a large decrease in $\Delta H^{0\ddagger}_f$ (6.68 kcal/mol in the wild-type protein vs −1.84 kcal/mol in the C11A/C27S variant) which leads an overall small increase in $\Delta G^{0\ddagger}_f$ (Table 3). In the C45A/C73A variant, $\Delta H^{0\ddagger}_f$ is increased strongly, and $T\Delta S^{0\ddagger}_f$ increases slightly, leading to a larger change in $\Delta G^{0\ddagger}_f$ than observed in the C11A/C27S variant (Table 3).

The temperature dependence of the unfolding reactions was monitored to obtain information on the changes in ΔH^0, ΔS^0, and ΔC_p between the transition state and the native state. The data were analyzed in the same way as the refolding reactions described above. This analysis could, however, only be performed for the wild-type protein and the C11A/C27S variant. The pronounced kink in the GdmCl dependence of the unfolding reaction of the C45A/C73A variant (Figure 2B) leads to large uncertainties in m_u and consequently in k_u at 0 M GdmCl at higher temperatures. The results of the Eyring plots for the unfolding reaction (Figure 3B) show that $\Delta S^{0\ddagger}_u$ is nearly identical for the wild-type protein and the C11A/C27S variant whereas $\Delta H^{0\ddagger}_u$ is larger in the wild-type protein (Table 3).

DISCUSSION

We compare folding of wild-type tendamistat and of two single-disulfide variants. We have previously shown that wild-type tendamistat folds in a two-state manner (Schönbrunner et al., 1997). The good agreement between the ΔG^0 and the m_{eq} values obtained from equilibrium measurements and from kinetic data shows that the two-state mechanism is also valid for both single-disulfide variants (Table 1). They thus offer excellent systems to examine the nature of the transition state for an all β-sheet protein and to investigate the role of preformed correct tertiary contacts in folding of a fast folding protein.

Effect of Disulfide Replacements on Protein Stability. Replacements of each of the two disulfide bonds results in a large decrease in stability. The $\Delta\Delta G^0$ values for the C11A/C27A and the C45A/C73A mutants are 6.0 and 5.1 kcal/mol, respectively. These effects on protein stability are much larger than expected from the entropic stabilization of the unfolded state in the wild-type protein due to the disulfide bonds which is believed to be proportional to the loop size. It was estimated to be (Pace et al., 1988)

$$\Delta S_{conf} = -2.1 - (3/2)R \ln(n) \qquad (15)$$

with n being the number of residues in the looped formed by the disulfide bond. This would lead to a decrease in ΔG^0 of 3.1 kcal/mol for the C11A/C27S variant and of 3.6 kcal/mol for the C45A/C73A variant. The large deviations in ΔG^0 from the expected entropic stabilization of the unfolded state upon replacement of the disulfide bonds are probably due to additional contributions from enthalpic destabilization of the native state. Also enthalpic stabilization of the unfolded states of the single-disulfide variants due to increased hydrogen bonding to solvent may contribute to the observed strong destabilizing effect of the disulfide replacements (Doig & Williams, 1991). Calorimetric studies on the role of disulfide bonds in the stability of tendamistat have

Table 3: Activation Parameters for Tendamisat Folding[a]

tendamistat variant	$\Delta H^{0\ddagger}_f$ (kcal/mol)	$T\Delta S^{0\ddagger}_f$ (kcal/mol)	$\Delta C_{p,f}$ [(kcal/mol)/K]	$\Delta G^{0\ddagger}_f$ (kcal/mol)	$\Delta H^{0\ddagger}_u$ (kcal/mol)	$T\Delta S^{0\ddagger}_u$ (kcal/mol)	$\Delta C_{p,u}$ [(kcal/mol)/K]	$\Delta G^{0\ddagger}_u$ (kcal/mol)
wild type	6.68 ± 0.06	-8.36 ± 0.06	-0.49 ± 0.01	15.04 ± 0.12	28.80 ± 1.49	5.36 ± 1.40	0.60 ± 0.03	23.44 ± 2.92
C11A/C27S	-1.84 ± 0.13	-18.07 ± 0.13	-0.57 ± 0.04	16.23 ± 0.26	23.46 ± 0.28	5.13 ± 0.28	0.37 ± 0.003	18.33 ± 0.56
C45A/C73A	10.77 ± 0.06	-6.48 ± 0.06	-0.39 ± 0.02	17.25 ± 0.12				

[a] The data are given for pH 7.0, 25 °C, and were determined from the temperature dependence of the refolding and unfolding reactions. The values represent the results of nonlinear least-squares fits of the data shown in Figure 3A,B to eq 14. The subscripts f and u denote the parameters for the folding reaction and the unfolding reaction, respectively.

also shown that deletion of the 11−27 disulfide affects the stability more than the 45−73 disulfide, even though the loop connected by it is shorter (Vogl et al., 1995). The changes in stability obtained from calorimetric data extrapolated to 25 °C are 5.0 kcal/mol for the C11A/C27S variant and 3.5 kcal/mol for the C45A/C73A variant. These values are smaller than those obtained from the GdmCl-induced unfolding curves at 25 °C. One reason for this discrepancy might be that calorimetric data were extrapolated from 55 to 25 °C, which depends strongly on ΔC_p. The ΔC_p values obtained in calorimetric measurements on tendamistat have quite large errors, especially for the C11A/C27S variant, which could only be measured over a small pH range (Vogl et al., 1995). In this case, the ΔC_p value had to be taken directly from the calorimetric curve. Additionally, the native base line in the GdmCl-induced unfolding transitions is not well-defined for the single-disulfide variants (Figure 2A) which can lead to errors in the determination of ΔG^0. However, the thermodynamic parameters obtained from the GdmCl-induced equilibrium transitions agree well with the values determined from the kinetic data (Table 1).

In addition to the large decrease in stability, both single-disulfide variants show a large increase in the m_{eq} value, which reflects the changes in solvent-accessible surface area upon unfolding. Based on the native structure of the protein, the change in solvent-accessible surface area upon unfolding of tendamistat is estimated to be 6000 Å^2, which should give an m value of 2.1 (kcal/mol)/M (Myers et al., 1995). Wild-type tendamistat has a significantly smaller m value of 1.28 (kcal/mol)/M, which was interpreted as residual structure in the unfolded chain (Schönbrunner et al., 1997). The C11A/C27S mutant has an m_{eq} of 1.85 (kcal/mol)/M [$\Delta m_{eq} = -0.58$ (kcal/mol)/M], and the C45A/C73A variant has an m value of 1.70 (kcal/mol)/M [$\Delta m_{eq} = -0.43$ (kcal/mol)/M], suggesting that both variants have significantly less residual structure in the unfolded state.

The addition of the effects of the two mutations would give an m_{eq} value of 2.25 (kcal/mol)/M for a completely reduced protein, which is not able to fold to a stable native conformation. This value is close to the expected value, suggesting that the residual structures induced by the disulfide bond are independent of each other. This is to be expected since the disulfide bonds are not overlapping. The m_{eq} values of other small proteins which do not contain disulfide bonds are close to those of the single-disulfide variants of tendamistat; e.g., the m_{eq} value of the 89 amino acid protein chymotrypsin inhibitor 2 is 1.81 (kcal/mol)/M (Jackson & Fersht, 1991).

Effect of Disulfide Replacements on Folding. Comparison of the folding reaction of wild-type protein and the two single-disulfide mutants allows us to monitor interactions in well-defined regions of the protein during the folding process. As discussed above, replacement of either disulfide bond leads to large changes in the m_{eq} values, which are most likely caused by a loss of residual structure in the unfolded state of the single-disulfide variants. This gives us the unique opportunity not only to monitor changes in the energetics of the folding reaction but also to follow the degree of compactization (α values) in distinct parts of tendamistat in the folding process. The regions which can be monitored are those which form nonrandom structure in the unfolded state when the respective disulfide bond is intact.

The 45−73 disulfide bond is a rather global tertiary contact in the protein connecting two distant parts in the polypeptide sequence which are located in the two outer strands of the second β-sheet (Figure 1B). The α value for this variant therefore reflects the degree of compaction in the region of the second β-sheet. The α value of 0.55 shows that in the refolding reaction of the C45A/C73A variant, 55% of the accessibility gain in the unfolded state upon mutation is lost in the transition state. The overall accessibility change in the transition state of tendamistat folding derived from the m_u and m_f values of both the wild-type protein and the C45A/C73A variant is 63% [$=m_f/(m_f + m_u)$; Table 1], indicating that the region of the second β-sheet is slightly less compact in the transition state than the rest of tendamistat.

Determination of the activation parameters for the C45A/C73 variant shows that the replacement of the 45−73 disulfide bond has little effect on $\Delta S^{0\ddagger}_f$ but leads to a pronounced increase in $\Delta H^{0\ddagger}_f$ (Table 3). This suggests that in the wild-type protein the presence of the 45−73 disulfide bond leads to favorable interactions even in the unfolded state and thus enthalpically stabilizes the unfolded state. These interactions are not formed in the transition state of folding when the C45−C73 disulfide bond is not present. Thus, a largely unfavorable $\Delta H^{0\ddagger}_f$ is observed for the C45A/C73 variant compared to the wild-type protein. This view is supported by the almost unchanged value of $\Delta S^{0\ddagger}_f$ which suggests that the increase in chain entropy of the unfolded state upon replacement of the 45−73 disulfide bond is not compensated for in the transition state of folding. This, again, suggests that formation of the second β-sheet is not complete in the transition state of folding. Strand 1 and strand 3 do not seem to make contact until very late in the folding process, when the C45−C73 disulfide bond is not present.

The 11−27 disulfide bond is a rather local tertiary contact connecting the ends of a β-hairpin (Figure 1A). The residual structure in the unfolded state formed in the presence of this disulfide bond must therefore be located in the β-hairpin region. Studies on model peptides showed that this region of tendamistat has a tendency to form a hairpin loop even in the absence of the disulfide bond (Blanco et al., 1994). In peptides containing the 11−27 disulfide bond, the tendency

of the hairpin to form is enhanced as judged by changes in the CD spectrum upon oxidation of the disulfide bridge (Wildegger and Kiefhaber, unpublished results).

The C11A/C27S variant shows a strongly increased m_f value and a reduced m_u value (Table 1) compared to the wild-type protein. The transition state of this variant is 90% native-like in respect to its accessibility to solvent, and its α value is larger than 1. Thus, more than the increase in accessibility upon mutation is regained during the refolding reaction. This shows that the β-hairpin formed between residues 11 and 27 has become solvent inaccessible in the transition state of the folding reaction. The α value of greater than unity could indicate local structural changes in the transition state and/or in the structure of the native state. Local structural changes in the native state were also postulated from the large changes in ΔG^0 and ΔH^0 upon replacement of the 11−27 disulfide bond (Vogl et al., 1995).

Determination of $\Delta S^{0‡}_f$ and $\Delta H^{0‡}_f$ of the C11A/C27S variant reveals that major compensating energetic changes occur in the refolding reaction of this variant compared to the wild-type protein. The value of $\Delta S^{0‡}_f$ decreases strongly, indicating that the increased conformational entropy in the unfolded state upon replacement of the disulfide bond is lost in the transition state. The observed change in $T\Delta S^{0‡}_f$ is much larger than expected from changes in chain entropy upon replacement of the 11−27 disulfide bond (9.7 kcal/mol vs 3.1 kcal/mol), suggesting that side chain rotations may already be restricted in the transition state. This large effect on $\Delta S^{0‡}_f$ is very likely not caused by changes in the entropy of the solvent upon formation of the transition state in the C11A/C27S variant, since the burial of hydrophobic side chains upon formation of the transition state should lead to an increase in $\Delta S^{0‡}_f$. Taking this effect into account, the actual decrease in conformational entropy might be even larger than indicated by $\Delta S^{0‡}_f$. The large decrease in $\Delta S^{0‡}_f$ in the C11A/C27S variant is consistent with the results from the accessibility changes (α-values) and supports the finding that the β-hairpin between residues 11 and 27 is already formed in the transition state.

The strongly unfavorable effect of the replacement of the 11−27 disulfide bond on $\Delta S^{0‡}_f$ is opposed by a large decrease in $\Delta H^{0‡}_f$. Formation of the transition state actually has a negative $\Delta H^{0‡}_f$ in the C11A/C27S variant at 25 °C, indicating that the interactions in the transition state are more favorable than in the unfolded state. This large change in $\Delta H^{0‡}_f$ compared to the wild-type protein could be caused by favorable interactions in the unfolded state of the wild-type protein introduced by the residual structure in the hairpin region. These interactions are lost in the unfolded state of the C11A/C27S variant, but they seem to be regained in the transition state of the folding reaction, leading to the observed favorable $\Delta H^{0‡}_f$. Alternatively, the large changes in $\Delta H^{0‡}_f$ in the C11A/C27S variant could indicate favorable structural changes in the transition state. Changes in the structure of the transition state of the C11A/C27S variant would be compatible with the large changes in m_u and m_f as discussed above. The increased conformational freedom at the ends of the hairpin structure might allow the hairpin to optimize its side chain contacts and thus lead to a favorable $\Delta H^{0‡}_f$.

Comparison of the activation parameters for the unfolding reaction of the wild-type protein and of the C11A/C27S variant shows that the disulfide replacement has no effect on $\Delta S^{0‡}_u$ (Table 3). This supports the results from the refolding studies and shows that the conformational entropy gained upon mutation is completely compensated for in the transition state of folding, again arguing for the formation of the β-hairpin in the transition state. These results also rule out major entropic changes in the native state caused by the replacement of the C11−C27 disulfide bond. The increased rate constant of the unfolding reaction seems to be exclusively due to an enthalpic destabilization of the native state, which leads to the observed strong decrease in $\Delta H^{0‡}_u$ (Table 3).

Implications for β-Sheet Formation. Kinetic analysis of the single-disulfide variants of tendamistat shows that the two regions of the β-sheet structure monitored by the mutations form at different stages in refolding. Formation of the β-hairpin structure between residues Val12 and Gly26 occurs in the rate-limiting step in the folding process and seems to be complete in the transition state. This points to a crucial role of this hairpin in tendamistat folding. Even when the disulfide bond is replaced and the two ends of the hairpin are not forced to interact, this region forms a compact and energetically very favorable structure in the transition state. We do not know at present whether the formation of this hairpin represents a nucleation step in a nucleation/growth type of folding reaction.

Formation of the second β-sheet, in contrast, is not complete in the transition state of folding. The interactions of the outer strand with the rest of the second β-sheet seem to form mainly in the final steps of the folding process, after the transition state.

These results suggest that the transition state of β-sheet folding comprises mainly local interactions like β-hairpins. The formation of these structures is obviously energetically most favorable. This picture of tendamistat folding is consistent with theoretical considerations on β-sheet formation (Finkelstein, 1991). The interactions between strands I and II of the first β-sheet seem to be very strong in the transition state as seen by the favorable $\Delta H^{0‡}$, by the large decrease in $\Delta S^{0‡}_f$ in the C11A/C27S variant, and by the complete loss of the solvent accessibility in this region in the transition state. The magnitude of these effects suggests that extensive side chain interactions might already occur in the transition state.

Role of Preformed Correct Tertiary Contacts in Two-State Folding. Tendamistat is the first disulfide-bonded protein whose folding and unfolding reactions were shown to be two-state (Schönbrunner et al., 1997). The results of the disulfide variants thus offer the opportunity to determine the role of preformed tertiary contacts in the folding process of a fast two-state folder, without having to consider the effects of the mutations on the stability of folding intermediates.

The observed large changes in the unfolding rate constants, which are exclusively caused by a decreased $\Delta H^{0‡}_u$ in the C11A/C27S variant, indicate that interactions in the native protein at the locations of the cross-links are weakened by replacement of the disulfide bonds. This enthalpic destabilization of the native state is reflected in the large loss of stability upon the replacement of the disulfide bonds, which cannot be explained solely on the basis of entropic stabilization of the unfolded state. The enthalpic stabilization of the native state creates a high energy barrier for the unfolding reaction and leads to a high kinetic stability of the native state.

The rate constants of the refolding reactions are much less effected by the mutations than those of the unfolding reaction. This shows that preformed tertiary interactions in the unfolded state do not have a major rate-enhancing effect in the refolding process, even if they connect parts of the molecule which have to find each other in the transition state of folding, as in the case of the 11−27 disulfide bond. As shown by the detailed analysis of the energetics of the refolding reaction and of the unfolding reaction, the small change in $\Delta G^{0‡}_f$ in the C11A/C27S variant is a result of two large and opposing effects on $\Delta H^{0‡}_f$ and $\Delta S^{0‡}_f$. Similar kinds of entropy/enthalpy compensations have been found for the effect of disulfide bond replacements on the equilibrium stability in several proteins (Doig & Williams, 1991).

The effect of enthalpy/entropy compensation on the activation parameters of the folding reactions can be explained on the basis of residual structure in the unfolded state introduced by the disulfide bonds. The residual structure leads to an unfavorable entropy in the unfolded state, but it also introduces interactions in the unfolded state which seem to be enthalpically favorable. If the structural element which is stabilized by a disulfide bond is folded in the transition state, the presence of the disulfide bond reduces the loss of chain entropy upon formation of the transition state and will thus have favorable effects on $\Delta S^{0‡}_f$. However, at the same time, formation of this structural element will contribute less to $\Delta H^{0‡}$, since many of the interactions are already present in the unfolded state.

These considerations suggest that introducing preformed tertiary interactions between parts of the unfolded chain which have to interact in the transition state of folding will favor the folding reaction by decreasing the loss of chain entropy but it will at the same time not allow the folding chain to gain conformational enthalpy upon formation of the transition state since many of the favorable interactions are already formed in the unfolded state. As a result, the preformed correct interactions will have little effect on the rate of protein folding.

ACKNOWLEDGMENT

We thank Buzz Baldwin and Annett Bachmann for comments on the manuscript and Josef Wey for experimental help.

REFERENCES

Abkevich, V. I., Gutin, A. M., & Shaknovich, E. I. (1994) *Biochemistry 33*, 10026−10036.
Alexander, P., Orban, J., & Bryan, P. (1992) *Biochemistry 31*, 7243−7248.
Aune, K. C., & Tanford, C. (1969) *Biochemistry 8*, 4586−4590.
Baldwin, R. L. (1995) *J. Biomol. NMR 5*, 103−109.
Blanco, F. J., Rivas, G., & Serrano, L. (1994) *Nat. Struct. Biol. 1*, 584−590.
Camacho, C. J., & Thirumalai, D. (1995) *Proteins: Struct., Funct., Genet. 22*, 27−40.
Chaffotte, A. F., Guillou, Y., & Goldberg, M. E. (1992) *Biochemistry 31*, 9694−9702.
Chan, C.-K., Hu, Y., Takahashi, S., Rousseau, D. L., Eaton, W. A., & Hofrichter, J. (1996) *Proc. Natl. Acad. Sci. U.S.A. 94*, 1779−1784.
Denton, M. E., Rothwarf, D. M., & Scheraga, H. (1994) *Biochemistry 33*, 11225−11236.
Doig, A. J., & Williams, D. H. (1991) *J. Mol. Biol. 217*, 389−98.
Eyring, H. (1935) *J. Chem. Phys. 3*, 107−115.
Fersht, A. R., Matouschek, A., & Serrano, L. (1992) *J. Mol. Biol. 224*, 771−782.
Finkelstein, A. V. (1991) *Proteins: Struct., Funct., Genet. 9*, 23−27.
Flory, P. J. (1956) *J. Am. Chem. Soc. 78*, 5222−5235.
Gruenewald, B., Nicola, C. U., Lustig, A., & Schwarz, G. (1979) *Biophys. Chem. 9*, 137−147.
Haas-Lauterbach, S., Scharf, M., Sprunkel, B., Neeb, M., Koller, K.-P., & Engels, J. (1993) *Appl. Microbiol. Biotechnol. 38*, 719−727.
Huang, G. S., & Oas, T. G. (1995) *Proc. Natl. Acad. Sci. U.S.A. 92*, 6878−6882.
Itzhaki, L. S., Otzen, D. E., & Fersht, A. R. (1995) *J. Mol. Biol. 254*, 260−288.
Jackson, S. E., & Fersht, A. R. (1991) *Biochemistry 30*, 10428−10435.
Kiefhaber, T., Kohler, H. H., & Schmid, F. X. (1992) *J. Mol. Biol. 224*, 217−229.
Kiefhaber, T., Bachmann, A., Wildegger, G., & Wagner, C. (1997) *Biochemistry 36*, 5108−5112.
Kline, A. D., & Wüthrich, K. (1985) *J. Mol. Biol. 183*, 503−507.
Kline, A. D., Braun, W., & Wüthrich, K. (1988) *J. Mol. Biol. 204*, 675−724.
Kramers, H. A. (1940) *Physica 4*, 284−304.
Kraulis, P. (1991) *J. Appl. Crystallogr. 24*, 946−950.
Lin, S. H., Konishi, Y., Nall, B. T., & Scheraga, H. A. (1985) *Bochemistry 24*, 2680−2686.
Mücke, M., & Schmid, F. X. (1994) *Biochemistry 33*, 14608−14619.
Myers, J. K., Pace, C. N., & Scholtz, J. M. (1995) *Protein Sci. 4*, 2138−2148.
Pace, C. N., Grimsley, G. R., Thomson, J. A., & Barnett, B. J. (1988) *J. Biol. Chem. 263*, 11820−11825.
Pflugrath, J., Wiegand, I., Huber, R., & Vértesy, L. (1986) *J. Mol. Biol. 189*, 383−386.
Santoro, M. M., & Bolen, D. W. (1988) *Biochemistry 27*, 8063−8068.
Schindler, T., Herrler, M., Marahiel, M. A., & Schmid, F. X. (1995) *Nat. Struct. Biol. 2*, 663−673.
Schönbrunner, N., Koller, K.-P., & Kiefhaber, T. (1997) *J. Mol. Biol. 268*, 526−538.
Thirumalai, D. (1994) in *Statistical Mechanics, Protein Structure, and Protein Substrate Interactions* (Doniach, S., Ed.) pp 115−134, Plenum Press, New York.
Tsong, T. Y., Baldwin, R. L., & McPhee, P. (1972) *J. Mol. Biol. 63*, 453−457.
Vértesy, L., Oeding, V., Bender, R., Zepf, K., & Nesemann, G. (1984) *Eur. J. Biochem. 141*, 505−512.
Viguera, A. R., Martínez, J. C., Filimonov, V. V., Mateo, P. L., & Serrano, L. (1994) *Biochemistry 33*, 2142.
Villegas, V., Azuaga, A., Catasus, L., Reverter, D., Mateo, P. L., Aviles, F. X., & Serrano, L. (1995) *Biochemistry 34*, 15105−15110.
Vogl, T., Brengelmann, R., Hinz, H.-J., Scharf, M., Lötzbeyer, M., & Engels, W. (1995) *J. Mol. Biol. 254*, 481−496.
Wetlaufer, D. B. (1973) *Proc. Natl. Acad. Sci. U.S.A. 70*, 697−701.
Williams, S., Causgrove, T. P., Gilmanshin, R., Fang, K. S., Callender, R. H., Woodruff, W. H., & Dyer, R. B. (1996) *Biochemistry 35*, 691−697.
Wolynes, P. G., Onuchic, J. N., & Thirumalai, D. (1995) *Science 267*, 1619−1620.

BI970594R